

## Raman scattering for triangular lattices spin-1/2 Heisenberg antiferromagnets

This article has been downloaded from IOPscience. Please scroll down to see the full text article.

2007 J. Phys.: Condens. Matter 19 145243

(<http://iopscience.iop.org/0953-8984/19/14/145243>)

View [the table of contents for this issue](#), or go to the [journal homepage](#) for more

Download details:

IP Address: 129.252.86.83

The article was downloaded on 28/05/2010 at 17:31

Please note that [terms and conditions apply](#).

# Raman scattering for triangular lattices spin-1/2 Heisenberg antiferromagnets

F Vernay<sup>1,2</sup>, T P Devereaux<sup>1,2</sup> and M J P Gingras<sup>1,3</sup>

<sup>1</sup> Department of Physics, University of Waterloo, Waterloo, ON, N2L 3G1, Canada

<sup>2</sup> PITP, University of British Columbia, Vancouver, BC, V6T 1Z1, Canada

<sup>3</sup> Department of Physics and Astronomy, University of Canterbury, Christchurch 8020, New Zealand

E-mail: [vernay@lorax.uwaterloo.ca](mailto:vernay@lorax.uwaterloo.ca)

Received 3 August 2006

Published 23 March 2007

Online at [stacks.iop.org/JPhysCM/19/145243](http://stacks.iop.org/JPhysCM/19/145243)

## Abstract

Motivated by various spin-1/2 compounds like  $\text{Cs}_2\text{CuCl}_4$  or  $\kappa\text{-(BEDT-TTF)}_2\text{Cu}_2(\text{CN})_3$ , we derive a Raman-scattering operator *à la* Shastry and Shraiman for various geometries. For  $T = 0$ , the exact spectra are computed by the Lanczos algorithm for finite-size clusters. We perform a systematic investigation as a function of  $J_2/J_1$ , the exchange constant ratio: ranging from  $J_2 = 0$ , the well known square-lattice case, to  $J_2/J_1 = 1$  the isotropic triangular lattice. We discuss the polarization dependence of the spectra and show how it can be used to detect precursors of the instabilities of the ground state against quantum fluctuations.

(Some figures in this article are in colour only in the electronic version)

## 1. Introduction

Highly frustrated magnetic systems are highly susceptible to quantum spin fluctuations and instabilities towards competing ground states. The triangular Heisenberg antiferromagnet with spin  $S = 1/2$  constitutes a paradigm of that class of system. In that context, it is interesting that experimental investigations of the  $\text{Cs}_2\text{CuCl}_4$  [1] and  $\kappa\text{-(BEDT-TTF)}_2\text{Cu}_2(\text{CN})_3$  [2] materials, which can both be described as a first approximation by a triangular lattice with spatially anisotropic exchange couplings, indicate exotic behaviours. Exotic behaviours include either the realization of a spin-liquid ground state or a magnetically ordered phase with a magnetic excitation dispersion strongly renormalized compared to the classical spin-wave. Indeed, recent numerical studies based on series expansion [3] have found that frustration manifests itself rather directly in the spin excitations of archetype models of two-dimensional frustrated spin systems. A softening of the magnon excitations in a broad region of the reciprocal  $q$  space is observed as a quantity,  $f$ , which parameterizes the level of frustration, is increased. Since, within a semi-classical picture, the effect of frustration is to bring about the effect of competing

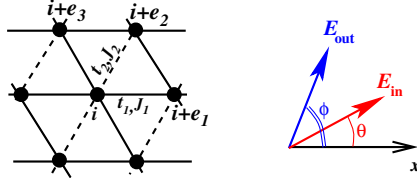


**Figure 1.** Geometry of the lattice and polarization vectors. Left: the dashed lines represent the coupling  $J_2$ , and the thick lines are for the exchange coupling  $J_1$ . Right: definition of the polarization vectors by two angles  $\phi$  and  $\theta$ .

ground states, it is expected that the spin excitations out of a semi-classical long-range ordered ground state are direct tell-tale indicators of the presence of frustrating interactions. In this paper we explore the possibility that frustration can also be investigated via the two-magnon density of states at zero wavevector measured by polarized inelastic magnetic Raman scattering.

The rest of this paper is organized as follows. In the first section we present the derivation of the scattering operator, then we discuss its form for various polarizations. In the last part we present the associated Raman spectra obtained by exact-diagonalization of finite-size clusters.

## 2. Scattering operator

We first consider the Hubbard model on the anisotropic triangular lattice:

$$\mathcal{H} = \mathcal{H}_K + \mathcal{H}_U = \sum_{(i,j),\sigma} t_{ij} \left( c_{i,\sigma}^\dagger c_{j,\sigma} + \text{h.c.} \right) + U \sum_i n_{i,\uparrow} n_{i,\downarrow} \quad (1)$$

where  $t_{ij}$  is the hopping from a site  $i$  to a neighbouring site  $j$ ,  $\sigma$  is the spin degree of freedom, and  $c$  and  $c^\dagger$  are the usual annihilation and creation operators. For the case considered here, there are two distinct hopping integrals,  $t_1$  and  $t_2$ , along the corresponding directions shown in figure 1.

At half-filling and in the large- $U$  limit, the system is described (to second order in  $t/U$ ) by an effective spatially anisotropic Heisenberg Hamiltonian:

$$\mathcal{H}_{\text{eff}} = \sum_{(i,j)} J_{ij} \mathbf{S}_i \cdot \mathbf{S}_j \quad (2)$$

where the different exchange coupling along each direction is due to the difference in the hopping amplitude, i.e.  $J_1 = 4t_1^2/U$ ,  $J_2 = 4t_2^2/U$ .

Raman scattering consists of an incoming photon (of energy  $\omega_i$ ) scattered into an outgoing photon (of energy  $\omega_f$ ), involving different manifolds of electronic states having zero or one double-occupancy. These transitions depend on the polarizations (referred as  $\mathbf{E}_{\text{in}}$  and  $\mathbf{E}_{\text{out}}$ ) of the incoming and outgoing photons. Following the early work of Fleury and Loudon [4] and Shastry and Shraiman [5], we derive an effective scattering spin Hamiltonian describing this problem. The  $\alpha$ -component of the electronic hopping current operator is

$$j^\alpha(\mathbf{q}) = i \sum_{\mathbf{r}, \mathbf{v}=\pm(\mathbf{e}_1, \mathbf{e}_2, \mathbf{e}_3)} \left( \frac{\partial \epsilon_{\mathbf{k}}}{\partial k^\alpha} \right) e^{i\mathbf{q}\cdot(\mathbf{r}+\frac{\mathbf{v}}{2})} [c_\sigma^\dagger(\mathbf{r}+\mathbf{v})c_\sigma(\mathbf{r}) - c_\sigma^\dagger(\mathbf{r})c_\sigma(\mathbf{r}+\mathbf{v})] \quad (3)$$

where  $\mathbf{q} = \mathbf{k}_f - \mathbf{k}_i$  is the momentum transfer, and  $\epsilon_{\mathbf{k}}$  the band energy. In what follows we take the most general set of polarization vectors, as shown in the right panel of figure 1:

$$\begin{aligned} & \cos \phi \hat{x} + \sin \phi \hat{y} \\ & \cos \theta \hat{x} + \sin \theta \hat{y}. \end{aligned} \quad (4)$$

The Raman scattering process involves an energy transfer  $\Omega = \omega_f - \omega_i$ , the momentum transfer being set to zero. Therefore, we restrict ourselves to the assumption  $\mathbf{k}_f \approx \mathbf{k}_i \approx 0$ , and we have

$$\begin{aligned} \mathbf{j} \cdot \mathbf{E}_{\text{in}} &= i \cos \phi \left[ -t_1 (c_r^\dagger c_{r+e_1} - \text{h.c.}) - \frac{t_2}{2} (c_r^\dagger c_{r+e_2} - \text{h.c.}) + \frac{t_1}{2} (c_r^\dagger c_{r+e_3} - \text{h.c.}) \right] \\ &\quad - i \frac{\sqrt{3}}{2} \sin \phi \left[ t_2 (c_r^\dagger c_{r+e_2} - \text{h.c.}) + t_1 (c_r^\dagger c_{r+e_3} - \text{h.c.}) \right] \\ \mathbf{j} \cdot \mathbf{E}_{\text{out}} &= i \cos \theta \left[ -t_1 (c_r^\dagger c_{r+e_1} - \text{h.c.}) - \frac{t_2}{2} (c_r^\dagger c_{r+e_2} - \text{h.c.}) + \frac{t_1}{2} (c_r^\dagger c_{r+e_3} - \text{h.c.}) \right] \\ &\quad - i \frac{\sqrt{3}}{2} \sin \theta \left[ t_2 (c_r^\dagger c_{r+e_2} - \text{h.c.}) + t_1 (c_r^\dagger c_{r+e_3} - \text{h.c.}) \right]. \end{aligned} \quad (5)$$

The Raman scattering operator is given by the second-order formula,  $|i\rangle$  and  $|f\rangle$  being respectively the initial and final state,  $|\mu\rangle$  being an intermediate state:

$$\langle f | M_r | i \rangle = \sum_{\mu} \left[ \frac{\langle f | \mathbf{j} \cdot \mathbf{E}_{\text{out}} | \mu \rangle \langle \mu | \mathbf{j} \cdot \mathbf{E}_{\text{in}} | i \rangle}{\epsilon_{\mu} - \epsilon_i - \omega_i} + \frac{\langle f | \mathbf{j} \cdot \mathbf{E}_{\text{in}} | \mu \rangle \langle \mu | \mathbf{j} \cdot \mathbf{E}_{\text{out}} | i \rangle}{\epsilon_{\mu} - \epsilon_i + \omega_f} \right]. \quad (6)$$

Following the same algebra steps as in [5], and restricting  $|i\rangle$  and  $|f\rangle$  to the manifold of singly occupied states, and intermediate states  $|\mu\rangle$  to the manifold of one double occupancy, we use the identity  $\frac{1}{4} - \mathbf{S}_i \cdot \mathbf{S}_j = \sum_{\sigma, \sigma'} \frac{1}{2} c_{i,\sigma}^\dagger c_{j,\sigma} c_{j,\sigma'}^\dagger c_{i,\sigma'}$ , and obtain the scattering operator in terms of spin operators. We note that within our approach the total scattering operator only contains terms of the form

$$\mathcal{O}_v \propto \frac{t_v^2}{U} \mathbf{S}_i \cdot \mathbf{S}_{i+e_v}. \quad (7)$$

From equation (6) we find that the scattering Hamiltonian prefactors which will be in front of equation (7) depend on the polarization vectors orientation. These prefactors are proportional to the exchange coupling  $J$ ; therefore, in its general form, the total scattering operator will depend on both  $J_1$  and  $J_2$ .

### 3. Polarizations

The two angles  $\phi$  and  $\theta$  with respect to the  $x$ -axis (see figure 1) define the polarizations involved in the scattering process. Therefore the scattering operator depends on a projector  $\mathcal{P}_v(\theta, \phi)$  that defines the polarization set-up. The Raman operator takes the form

$$\begin{aligned} \mathcal{H}_{\text{LF}}(\theta, \phi) &\propto \sum_i \{ J_1 \mathbf{S}_i \cdot \mathbf{S}_{i+e_1} \cos \theta \cos \phi \\ &\quad + J_2 \mathbf{S}_i \cdot \mathbf{S}_{i+e_2} [\cos(\theta + \phi) + \sqrt{3} \sin(\theta + \phi) + 4 \sin \theta \sin \phi] \\ &\quad + J_1 \mathbf{S}_i \cdot \mathbf{S}_{i+e_3} [\cos(\theta + \phi) - \sqrt{3} \sin(\theta + \phi) + 4 \sin \theta \sin \phi] \} \end{aligned} \quad (8)$$

which can be written in the compact form

$$\mathcal{H}_{\text{LF}}(\theta, \phi) \propto \sum_{i,v} J_v \mathcal{P}_v(\theta, \phi) \mathbf{S}_i \cdot \mathbf{S}_{i+e_v}. \quad (9)$$

In order to compare with the square-lattice case, we now focus on the following polarization geometries:

$$\begin{aligned} \mathcal{H}_{\text{LF}}\left(\frac{5\pi}{6}, -\frac{\pi}{6}\right) &\propto \sum_i J_1 [\mathbf{S}_i \cdot \mathbf{S}_{i+e_1} + \mathbf{S}_i \cdot \mathbf{S}_{i+e_3}] \\ \mathcal{H}_{\text{LF}}\left(\frac{5\pi}{6}, \frac{\pi}{3}\right) &\propto \sum_i J_1 [\mathbf{S}_i \cdot \mathbf{S}_{i+e_1} - \mathbf{S}_i \cdot \mathbf{S}_{i+e_3}]. \end{aligned} \quad (10)$$

When the diagonal bond  $J_2$  is 0, the first line of equation (10) is the  $A_{1g}$  Raman operator, while the second line gives the  $B_{1g}$  Raman operator, both on a square lattice. Most importantly, we note that the scattering operators depend on the ratio  $J_1/J_2$  if one takes

$$\begin{aligned}\mathcal{H}_{\text{LF}}\left(\frac{\pi}{6}, -\frac{5\pi}{6}\right) &\propto \sum_i [J_1 \mathbf{S}_i \cdot \mathbf{S}_{i+\mathbf{e}_1} + J_2 \mathbf{S}_i \cdot \mathbf{S}_{i+\mathbf{e}_2}] \\ \mathcal{H}_{\text{LF}}\left(\frac{\pi}{6}, \frac{2\pi}{3}\right) &\propto \sum_i [J_1 \mathbf{S}_i \cdot \mathbf{S}_{i+\mathbf{e}_1} - J_2 \mathbf{S}_i \cdot \mathbf{S}_{i+\mathbf{e}_2}].\end{aligned}\tag{11}$$

We would like to draw the attention of the reader to the fact that the standard parallel polarization does not give a straightforward  $A_{1g}$ -like scattering operator as is the case for the square lattice, but a linear combination of equations (10) and (11).

#### 4. Results

As a first step in exploring the Raman scattering in the Heisenberg  $S = 1/2$  anisotropic triangular lattice antiferromagnet, we perform exact-diagonalizations for the Raman operator equation (9). While Raman scattering studies on triangular lattice compounds like cobaltites have been carried out [6], these have focused on phonons, and there are as yet no systematic study of polarization-dependent electronic Raman spectra. Hence, our aim at this stage is not to obtain a quantitative description of the scattering spectra for a specific material, but rather to identify the key qualitative features emerging in the Raman spectrum of the anisotropic triangular lattice, possibly to motivate Raman studies and to connect with recent neutron data [1], NMR [2] and angle-resolved photoemission [7]. Motivated by the successes of exact-diagonalization to identify the essential qualitative features of the Raman spectrum on the square lattice [8, 9], and in order to compare with these well-known results, we explore in this study the behaviour of a 16-site cluster as the frustrating  $J_2$  coupling is increased from zero. The results are summarized in figure 2. The general trend observed in these plots is that a softening progressively develops as the system becomes more frustrated. The bottom left panel of figure 2 shows, for  $J_2 = 0$ , the well known zero  $A_{1g}$  Raman scattering on a square lattice, since the scattering operator commutes with the Hamiltonian [9]. As  $J_2$  increases, the non-commuting contribution to the scattering intensity increases and the spectrum develops more structure. For the bottom right panel, a weak intensity is observed because the scattering operator does not commute with the Hamiltonian even for  $J_2 = 0$ .

From the Hamiltonian in equation (2), it is obvious that the ground state will depend on the ratio  $J_2/J_1$ , ranging from a Néel-like order on the square lattice when  $J_2 = 0$ , to a three sublattice long-range order for  $J_2 = J_1$  [10–12]. These different types of order are characterized by different magnon dispersions; therefore the Raman spectra are expected to depend on  $J_2/J_1$ . In a recent paper, Zheng *et al* [3] showed, using series expansions, that the magnon dispersion for the anisotropic triangular lattice Heisenberg model exhibits a *roton-like* minimum. This local minimum sits at the  $(\pi, 0)$  point for a square lattice with one diagonal bond and is getting softer as the  $J_2$ -diagonal frustrating coupling increases. In the case of the standard square lattice, for the  $B_{1g}$  channel with crossed polarizations, the electromagnetic field couples to excitations along the  $(\pi, 0)$  direction. We note from [3] that this softening is a multi-magnon process that cannot be captured to lowest order in a  $1/S$  expansion. However, since we are using exact-diagonalization which, by its nature, treats processes for the length scale considered exactly, we are able to detect indications of this softening. For specificity, consider the  $B_{1g}$  channel in the top left-hand panel of figure 2. A signature of the softening of the magnon excitation is clearly manifest as the frustration ratio  $f = J_2/J_1$  is increased from

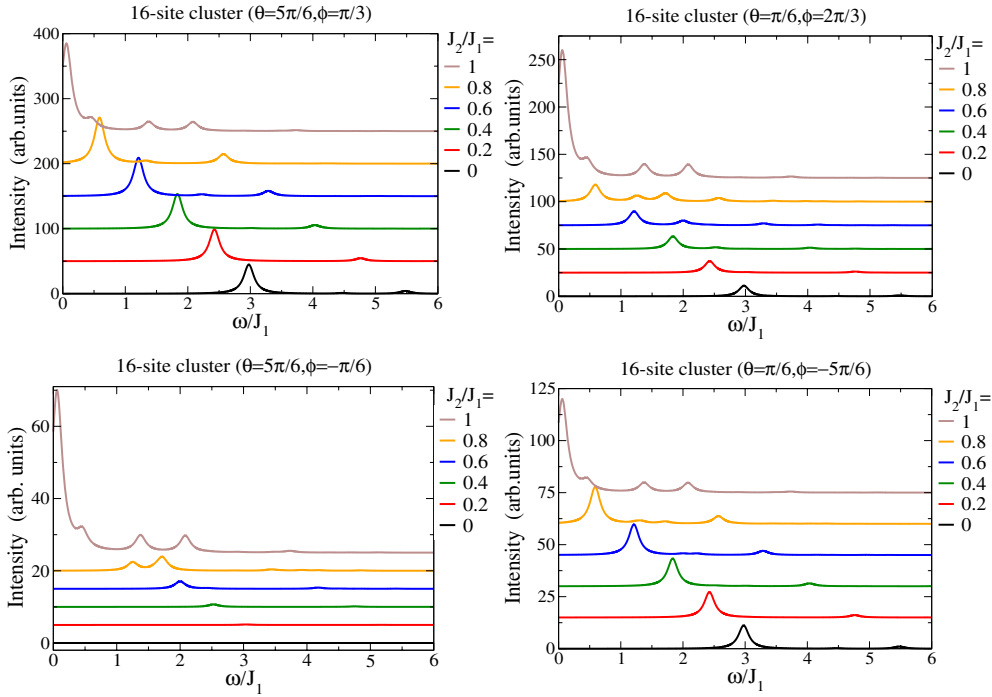


**Figure 2.** Exact diagonalizations on a 16-site cluster. Raman spectra for various values of  $(\theta, \phi)$  and  $J_2/J_1$ . The bottom (top) left panel would correspond to  $A_{1g}$  ( $B_{1g}$ ) polarization on the square lattice in the case  $J_2 = 0$ .

zero, with a shift of the spectral weight, and the main peak moving from  $\omega \approx 3J_1$  when  $J_2 = 0$  to  $\omega \approx 0.6J_1$  when  $J_2 = 0.8J_1$ .

## 5. Conclusions and perspectives

The results presented here show how frustration can dramatically alter the Raman spectrum of an otherwise non-frustrated system. In particular, we observe a frustration-driven *spectral downshift*, the landmark feature of frustrated systems. This shift is another indicator of the frustration-induced softening of the magnon dispersion recently predicted by others. From a strictly theoretical point of view, the analysis above sets the stage for a more complete approach. Some exact-diagonalizations on larger clusters and a spin-wave approach including magnon–magnon interactions, along the lines pursued for the square lattice [13, 14], are currently being carried out.

## Acknowledgments

Support for this work was provided by NSERC of Canada and the Canada Research Chair Program (Tier I) (MG), the Canada Foundation for Innovation, the Ontario Innovation Trust, and the Canadian Institute for Advanced Research (MG). MG acknowledges the University of Canterbury for an Erskine Fellowship and thanks the Department of Physics and Astronomy at the University of Canterbury, where part of this work was completed, for their hospitality.

**References**

- [1] Coldea R *et al* 2002 *Phys. Rev. Lett.* **88** 137203  
Coldea R *et al* 2003 *Phys. Rev. B* **68** 134424
- [2] Shimizu Y *et al* 2003 *Phys. Rev. Lett.* **91** 107001
- [3] Zheng W *et al* 2006 *Phys. Rev. Lett.* **96** 057201
- [4] Fleury P A and Loudon R 1968 *Phys. Rev.* **166** 514
- [5] Shastry B S and Shraiman B I 1991 *Int. J. Mod. Phys. B* **5** 365  
Shastry B S and Shraiman B I 1990 *Phys. Rev. Lett.* **65** 1068
- [6] Lemmens P *et al* 2006 *Phys. Rev. Lett.* **96** 167204
- [7] Qian D *et al* 2006 *Phys. Rev. Lett.* **96** 216405
- [8] Sandvik A W, Capponi S, Poilblanc D and Dagotto E 1998 *Phys. Rev. B* **57** 8478
- [9] Freitas P J and Singh R R P 2000 *Phys. Rev. B* **62** 5525
- [10] Weihong Z, McKenzie R H and Singh R R P 1999 *Phys. Rev. B* **59** 14367
- [11] Chung C H, Marston J B and McKenzie R H 2001 *J. Phys.: Condens. Matter* **13** 5159
- [12] Bernu B, Lhuillier C and Pierre L 1994 *Phys. Rev. B* **50** 10048
- [13] Canali C M and Girvin S M 1992 *Phys. Rev. B* **45** 7127
- [14] Chubukov A V and Frenkel D M 1995 *Phys. Rev. B* **52** 9760